Design of an easy tunable soft sensor for real-time speed and position estimation of PMSM

Ines Omrane

***Abstract*— This paper deals with the design of a speed soft sensor for permanent magnet synchronous motor. At high speed, an easy tunable model-based soft sensor is used and it gives excellent results. However, it fails to deliver satisfactory performance at zero or very low speed. High-frequency soft sensor is used at low speed. We suggest to use a model-based soft sensor together with the high-frequency soft sensor to overcome the limitations of the first one at low speed range.**

***Index Terms*— Design, Simulation, Motor speed control, easy tunable soft sensor, Permanent magnet synchronous motor.**

I. INTRODUCTION

PMSM are receiving a very important attention in several industrial sectors because of its simplicity of design, ability of operation at high speeds, high efficiency and high power/ torque density. For this reason, the sensorless control of a synchronous machine has been an interesting topic. The main idea of this approach is to replace the mechanical sensor by a soft sensor which offers a number of attractive properties one of them being a low cost alternative to hardware speed measurement used in classical motor drives [1–3]. For example, the cost of a sensor may exceed the cost of a small motor in some applications. Also, the presence of the mechanical sensors not only increases the cost and complexity of the total material with additional wiring but also reduces its reliability with additional sensitivity to external disturbances. In addition, it may be difficult to install and maintain a position sensor due to the limited space and rigid work environment with high vibration or high temperature.

At high speed, model-based soft sensors give excellent results. Several techniques inspired from control theory [4–6], such as adaptive observers [7–10], reference models [11–13], and extended Kalman filter [14]. Whatever the chosen method is, the sensor design procedure can be summarized by Fig. 1 [15]. However, these methods fail to deliver satisfactory performance at zero or very low speed. From a practical standpoint, the operational limit of these methods is typically $\omega_N / 20$, with ω_N being the rated motor speed. So, high-frequency soft sensors are used in this velocity region. The estimated parameters are obtained from the carrier high frequency signal injection [16]. In most of these methods, a signal, which can be either a current or a voltage, is injected in the $(\alpha - \beta)$ or $(d - q)$components.

Ines Omrane, University of Poitiers, Laboratoire d'Informatique et d'Automatique pour les Systèmes, Poitiers, France.

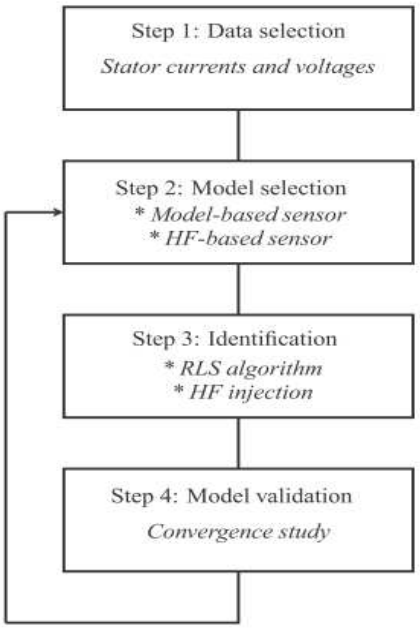

Fig. 1. Soft sensor development.

These techniques are usually applied to the interior permanent magnet synchronous motor (I-PMSM) as it involves the effect of salience [17]. In [18,19], signal injection method was extended to the surface permanent magnet synchronous motor (S-PMSM) by exploiting the saliency resulting from magnetic saturation.

An attractive solution is to combine the two sensors to obtain a full-speed range operation. Several hybrid method have been presented in the literature [20–25]. In [21,22], the changeover algorithm was performed using weighting coefficients. A linear combination between the position estimates at high and low speeds was used in [23] to get a smooth transition. In [24], the method of transition consists in using a weighted average of the estimated speed and position in a given speed gap. In [25], the incorporation of the HF quantities estimates in the flux observer allowed a smooth transition and an improvement of the feedback signal quality.

To ensure that model-based soft sensor works properly, the PMSM model and its parameters must be known. For this, a sensorless parameter identification is required. In this paper, a simple identification procedure, based on HF signal injection and exploiting the implementation of state variable filters which replace the band-pass filters, used in the HF signal injection technique, to obtain a linear model with respect to the parameters is used. Thus, a least squares algorithm is applied to identify the model parameters.

In this paper, we suggest to use an easy tunable soft sensor together with the high-frequency soft sensor to overcome the limitations of the first one at low speed range. A simple identification procedure based on HF signal injection and exploiting the implementation of state variable filters is developed. In order to validate the proposed soft sensor, we provide several simulation results to assess the relevancy of the proposed solution. The main interest of this soft sensor is its simplicity, which makes it a suitable candidate for practical implementation.

Appropriate assumptions allow us to neglect nonlinear effects as saturations, iron losses or magnetic hysteresis in order to derive a simplified physical model. It yields a good approximation of the motor behaviour which is sufficient for control objectives. The identification step concerns the determination of model parameters. In Section 3, the general formulation of the recursive least squares algorithm is shown. The final step towards the identification is the validation (Section 4). This phase requires us to verify whether the model is able to adequately represent the system. If the validation test fails, the soft sensor design should be reconsidered.

II. MODEL SELECTION

A. *Motor model*

The PMSM considered in this study has a stator composed of a three-phase winding represented by the three axes (a, b, c) phase-shifted with respect to one another by an electrical angle of 120° and a rotor having *p* pole pairs. To simplify the modeling of the machine, we adopt the usual simplifying assumptions given in the majority of references [26].

- The stator windings are symmetrical and have a perfect sinusoidal distribution along the air gap.
- The permanence of the magnetic paths on the rotor is independent of the rotor positions.
- Saturation and hysteresis effects are inexistent.

The PMSM can be modeled in the *dq* reference frame fixed to the rotor by the following set of equations

$$u_d = R_s i_d + L_d \frac{di_d}{dt} - \omega_e L_q i_q \qquad (1)$$

$$u_q = R_s i_q + L_q \frac{di_q}{dt} + \omega_e L_d i_d + \omega_e \psi_{pm} \qquad (2)$$

A third equation that corresponds to the assumption of constant speed can be added to (14) and (15): $\dot{\omega}_e = 0$.

Let $x = \begin{bmatrix} i_d & i_q & \omega_e \end{bmatrix}^T$, $u = \begin{bmatrix} u_d & u_q \end{bmatrix}^T$ and $y = \omega_e$.

The state-space representation of the PMSM model can be written as:

$$\begin{cases} \dot{x} = \begin{bmatrix} -\frac{R_s}{L_d} & \frac{L_q}{L_d}\omega_e & 0 \\ -\frac{L_d}{L_q}\omega_e & -\frac{R_s}{L_q} & -\frac{\psi_{pm}}{L_q} \\ 0 & 0 & 0 \end{bmatrix} x + \begin{bmatrix} \frac{1}{L_d} & 0 \\ 0 & \frac{1}{L_q} \\ 0 & 0 \end{bmatrix} u \\ y = \begin{bmatrix} 0 & 0 & 1 \end{bmatrix} x \end{cases} \qquad (3)$$

B. *Sensor model*

To simplify the writing, we will use the following notations:

$$a_d = \frac{R_s}{L_d}, a_q = \frac{R_s}{L_q}, b = \frac{\psi_{pm}}{L_q}, c_d = \frac{L_q}{L_d}, c_q = \frac{L_d}{L_q}, l_d = \frac{1}{L_d}, l_q = \frac{1}{L_q}$$

Based on the model of PMSM given by (3), we can write the state space representation of the machine follows:

$$\begin{cases} \dot{x} = \begin{bmatrix} -a_d & c_d\omega_e & 0 \\ -c_q\omega_e & -a_q & -b \\ 0 & 0 & 0 \end{bmatrix} x + \begin{bmatrix} l_d & 0 \\ 0 & l_q \\ 0 & 0 \end{bmatrix} u \\ y = \begin{bmatrix} 0 & 0 & 1 \end{bmatrix} x \end{cases} \qquad (4)$$

In this model, ω_e plays both the role of a state variable and a parameter appearing in the dynamical matrix. However, in the case of a sensorless control, the speed is not measured and only the currents i_d and i_q are accessible to measurement. Hence, the state space representation can be given by the following equation

$$\begin{cases} \dot{\breve{x}} = \breve{A}\breve{x} + \breve{B}u \\ y_{mes} = \breve{C}x + D_{mes}u \end{cases} \qquad (5)$$

where

$$\breve{x} = x = \begin{bmatrix} x_1 & x_2 \end{bmatrix}, \; y_{mes} = x_1, \; \breve{A} = \begin{bmatrix} \breve{A}_{11} & \breve{A}_{12} \\ \breve{A}_{21} & \breve{A}_{22} \end{bmatrix},$$

$$\breve{B} = \begin{bmatrix} \breve{B}_1 & \breve{B}_2 \end{bmatrix}, C_{mes} = \breve{C} = \begin{bmatrix} 1 & 0 & 0 \\ 0 & 1 & 0 \end{bmatrix}, D_{mes} = \breve{D} = 0$$

The state vector $\breve{x}$ in (5) can be divided into two sub-vectors: $\breve{x}_1 = x_1$ and $\breve{x}_2 = x_2 = \omega_e$.

So

$$\breve{A}_{11} = \begin{bmatrix} -a_d & c_d\omega_e \\ -c_q\omega_e & -a_q \end{bmatrix}, \breve{A}_{12} = \begin{bmatrix} 0 \\ -b \end{bmatrix}, \breve{B}_1 = \begin{bmatrix} l_d & 0 \\ 0 & l_q \end{bmatrix}$$

$$\breve{A}_{21} = \begin{bmatrix} 0 & 0 \end{bmatrix}, \breve{A}_{22} = 0, \breve{B}_2 = 0$$

Therefore, it is necessary to observe $\breve{x} = \begin{bmatrix} \breve{x}_1^T & \breve{x}_2^T \end{bmatrix}^T$ with $\breve{x}_1 \in R^m$, $\breve{x}_2 \in R^q$ and $q = n - m$. In general, we must reconstruct

$$\chi = Sx = S_1x_1 + S_2x_2 = S\breve{M}\breve{x} = \breve{S}_1\breve{x}_1 + \breve{S}_2\breve{x}_2 \qquad (6)$$

where

$$SM = S = \begin{bmatrix} S_1 & S_2 \end{bmatrix} \quad (7)$$

Equation (5) leads to

$$\begin{cases} \dot{x}_2 = A_{22}x_2 + \begin{bmatrix} A_{21} & B_2 \end{bmatrix} \begin{bmatrix} x_1 \\ u \end{bmatrix} \\ \dot{x}_1 = A_{12}x_2 + \begin{bmatrix} A_{11} & B_1 \end{bmatrix} \begin{bmatrix} x_1 \\ u \end{bmatrix} \end{cases} \quad (8)$$

where

$$A_{22} = A, \quad \begin{bmatrix} A_{21} & B_2 \end{bmatrix} = B, \quad A_{12} = C,$$

$$\begin{bmatrix} A_{11} & B_1 \end{bmatrix} = D, \quad \dot{x}_1 = y, \quad \begin{bmatrix} x_1 \\ u \end{bmatrix} = u.$$

The Luenberger observer has the following structure:

$$\begin{cases} \dot{z} = Fz + Py + Ru \\ \hat{\chi} = Lz + Qy + Gu \end{cases} \quad (9)$$

where $z \in R^q$. The observability of $(A, C) = (A_{22}, A_{12})$ is a necessary and sufficient condition for the existence of this observer. If (A, C) is observable then so is (A_{22}, A_{12}).

Indeed

$$rank\begin{bmatrix} C \\ (\lambda I - A) \end{bmatrix} = rank\begin{bmatrix} I_m & 0 \\ (\lambda I_m - A_{11}) & A_{12} \\ A_{21} & (\lambda I_q - A_{22}) \end{bmatrix} = n \ \forall \lambda \in C$$

$$\Rightarrow rank\begin{bmatrix} A_{12} \\ (\lambda I_q - A_{22}) \end{bmatrix} = q \ \forall \lambda \in C$$

Luenberger's idea is to design the observer so as to satisfy $z = T\hat{x}$ with $\hat{x} = \begin{bmatrix} x_1^T & \hat{x}_2^T \end{bmatrix}^T$ is a reconstruction of x composed of x_1 and $\hat{x}_2$: ($\hat{x}_2$ a reconstruction of x_2). The matrix T can be divided as follows:

$$T = \begin{bmatrix} Z & T \end{bmatrix} \quad (10)$$

such that

$$z = T\hat{x}_2 + Zx_1 = Tx_2 + Zx_1 + \mu$$

where

$$\mu = T\varepsilon_2 = T(\hat{x}_2 - x_2)$$

So, we have

$$\dot{\mu} = F\mu + (FT - TA + PC - ZC)x_2 + (R + PD - TB - ZD + F\begin{bmatrix} Z & 0 \end{bmatrix})u \quad (11)$$

To ensure the asymptotic convergence of z to Tx we must satisfy the following constraints

$$\begin{cases} F \text{ is stable}, \\ FT - TA + (P - Z)C = FT - TA_{22} + (P - Z)A_{12} = 0, \\ R + (P - Z)D - TB + \begin{bmatrix} Z & 0 \end{bmatrix} = 0. \end{cases} \quad (12)$$

Under these constraints, μ tends to 0 and thus $T\hat{x}_2$ tends to Tx_2. The third equation in (9) can be rewritten as:

$$\begin{cases} R_1 - TA_{12} + (P - Z)A_{11} + FZ = 0 \\ R_2 - TB_2 + (P - Z)B_1 = 0 \end{cases} \quad (13)$$

where $R = \begin{bmatrix} R_1 & R_2 \end{bmatrix}$.

Moreover, the real goal is to rebuild χ. The static equation in (9) leads to

$$\hat{\chi} = LTx_2 + LZx_1 + L\mu + QCx_2 + QDu + Gu$$

$$\Leftrightarrow \hat{\chi} = (QC + LT)x_2 + (\begin{bmatrix} LZ & 0 \end{bmatrix} + QD + G)u + L\mu$$

To ensure an efficient reconstruction in the steady state such that $\lim_{t \to \infty} \mu(t) = 0$, we must ensure that

$$\lim_{t \to \infty} ((QC + LT)x_2 + (\begin{bmatrix} LZ & 0 \end{bmatrix} + QD + G)u) = S_1x_1 + S_2x_2$$

Let $G = \begin{bmatrix} G_1 & G_2 \end{bmatrix}$, then we have

$$\begin{cases} QC + LT = S_2 \\ \begin{bmatrix} LZ & 0 \end{bmatrix} + QD + G = 0 \end{cases}$$

In other terms, we must satisfy the following constraints:

$$\begin{cases} QA_{12} + LT = S_2 \\ LZ + QA_{11} + G_1 = S_1 \\ QB_1 + G_2 = 0 \end{cases} \quad (14)$$

These constraints, given by equation (12) and equation (14) may be difficult to verify both from computational and practical point of views, so we set the following arbitrary choice: $T = I_q$, $P = 0$ and $Q = 0$.

So $z = Zx_1 + \hat{x}_2$ and

$$\begin{cases} F = A + ZC = A_{22} + ZA_{12} \\ R = \begin{bmatrix} A_{21} + ZA_{11} - (A_{22} + ZA_{12})Z & B_2 + ZB_1 \end{bmatrix} \\ L = S_2 \\ G = \begin{bmatrix} S_1 - S_2Z & 0 \end{bmatrix} \end{cases}$$

The Luenberger observer is then given by

$$\begin{cases} \dot{z} = F z + P y_{mes} + R u \\ \hat{\chi} = L z + Q y_{mes} + G u \end{cases} \quad (15)$$

where

$$\begin{cases} F = \breve{F} = \breve{A}_{22} + Z\breve{A}_{12} \\ P = \breve{R}_1 = \breve{A}_{21} + Z\breve{A}_{11} - \left(\breve{A}_{22} + Z\breve{A}_{12}\right)Z \\ R = \breve{R}_2 - \breve{R}_1\breve{D} = \breve{B}_2 + Z\breve{B}_1 - \left(\breve{A}_{21} + Z\breve{A}_{11} - \left(\breve{A}_{22} + Z\breve{A}_{12}\right)Z\right)\breve{D} \\ L = \breve{L} = \breve{S}_2 \\ Q = \breve{G}_1 = \breve{S}_1 - \breve{S}_2 Z \\ G = -\breve{G}_1\breve{D} = \left(\breve{S}_2 Z - \breve{S}_1\right)\breve{D} \end{cases} \quad (13)$$

It comes then to determine a reduced observer by assuming that $\chi = \omega_e$ which leads to $\breve{S}_1 = \begin{bmatrix} 0 & 0 \end{bmatrix}$ and $\breve{S}_2 = 1$. It should be noted that $\left(\breve{A}_{22}, \breve{A}_{12}\right)$ is observable. Let Z be expressed as $Z = \begin{bmatrix} \alpha_1 & \alpha_2 \end{bmatrix}$. Based on the previous result, we have

$$\begin{cases} F = -\dfrac{\alpha_2 \psi_{pm}}{L_q} \\ P = \begin{bmatrix} -\alpha_1 a_d - \alpha_2 c_q \omega_e + \alpha_1\alpha_2 b & \alpha_1 c_d \omega_e - \alpha_2 a_q + \alpha_2^2 b \end{bmatrix} \\ R = \begin{bmatrix} \alpha_1 l_d & \alpha_2 l_q \end{bmatrix} \\ L = 1 \\ Q = \begin{bmatrix} -\alpha_1 & -\alpha_2 \end{bmatrix} \\ G = 0 \end{cases} \quad (14)$$

From the equation (9), we obtain

$$\begin{cases} \dot{z} = -\dfrac{\alpha_2 \psi_{pm}}{L_q} z + \left(-\alpha_1 \dfrac{R_s}{L_d} - \alpha_2 \dfrac{L_d}{L_q}\omega_e + \alpha_1\alpha_2 \dfrac{\psi_{pm}}{L_q}\right) i_d + \dfrac{\alpha_1}{L_d} u_d \\ \qquad + \left(\alpha_1 \dfrac{L_q}{L_d}\omega_e - \alpha_2 \dfrac{R_s}{L_q} + \alpha_2^2 \dfrac{\psi_{pm}}{L_q}\right) i_q + \dfrac{\alpha_2}{L_q} u_q \\ \hat{\omega}_e = z - \alpha_1 i_d - \alpha_2 i_q \end{cases} \quad (15)$$

In this particular observer, the reconstruction gap of the speed $\tilde{\omega}_e = \hat{\omega}_e - \omega_e$ is described by the following equation

$$\dot{\tilde{\omega}}_e = -\alpha_2 \frac{\psi_{pm}}{L_q} \tilde{\omega}_e = F \tilde{\omega}_e \quad (16)$$

Such a dynamic is characterized by only one pole: *F*.

Hence α_2 must be chosen positive for asymptotic of *F* and α_1 can be chosen equal to zero as it has no effect on this pole. This choice is due to the structure of the matrix $\breve{A}_{12}$ that present a null component. Therefore, α_1 can be taken zero which simplifies the expression of the observer.

In this analysis, the nonlinearity of the model is hidden by the fact that ω_e is also a parameter of the dynamic matrix. But this nonlinearity appears suddenly and causes a problem. The calculated observer depends on ω_e which is not measured. To implement it, we must replace, ω_e by $\hat{\omega}_e$ in the model of the observer, that is a reasonable approximation since the observer has converged. For this, we must choose the gain α_2 such as the bandwidth of the observer is both greater than the bandwidth of the speed controller and smaller than the current controller ($|\alpha_\omega| << |\alpha_O| < |\alpha_C|$). Hence, we obtain:

$$\begin{cases} \dot{z} = \dfrac{-\alpha_2 \psi_{pm}}{L_q} z - \alpha_2 \dfrac{L_d}{L_q}\hat{\omega}_e i_d + \left(-\alpha_2 \dfrac{R_s}{L_q} + \alpha_2^2 \dfrac{\psi_{pm}}{L_q}\right) i_q + \dfrac{\alpha_2}{L_q} u_q \\ \hat{\omega}_e = z - \alpha_2 i_q \end{cases} \quad (17)$$

The rotor position can be obtained by integration of the rotor speed:

$$\hat{\theta}_e(t) = \int_0^t \hat{\omega}_e(\tau) d\tau \quad (18)$$

III. IDENTIFICATION

To ensure that the previously presented sensor works properly the PMSM model and its parameters must be known. For this, a sensorless parameter identification is required. In the automotive application, electrical parameters of PMSM must be identified at standstill before the startup of the motor. The identification process should be fast and requiring a low computing power in order to be incorporated in an electric variator. This paper presents a simple method based on HF signal injection and exploiting the implementation of state variable filters to obtain a linear model with respect to the parameters. Thus, a simplified procedure of identification based on a least squares algorithm can be used to identify the stator resistance and the d- and q-axes inductances of the PMSM.

At standstill, the PMSM can be modeled by the following set of equations:

$$\begin{cases} \hat{u}_d = R_s i_d + L_d \dfrac{d\hat{i}_d}{dt}, \\ \hat{u}_q = R_s i_q + L_q \dfrac{d\hat{i}_q}{dt}. \end{cases} \quad (19)$$

By injecting a carrier high-frequency signal, the machine can be considered as a RL load given by the following equations:

$$\hat{u}_{d_H} = R_s \hat{i}_{d_H} + L_d \frac{d\hat{i}_{d_H}}{dt} \equiv z_d \hat{i}_{d_H} \quad (20)$$

$$\hat{u}_{q_H} = R_s \hat{i}_{q_H} + L_q \frac{d\hat{i}_{q_H}}{dt} \equiv z_q \hat{i}_{q_H} \quad (21)$$

where $\hat{u}_{d_H}$ and $\hat{u}_{q_H}$ are the stator voltages at HF, $\hat{i}_{d_H}$ and $\hat{i}_{q_H}$ are the stator currents at HF, z_d and z_q are the d- and q-axes impedances, respectively, ω_H is the frequency of the injected signal. For a sufficiently high frequency of injection,

it can be considered that the stator resistance impedance is negligible compared to the inductances impedances. Then

$$z_d = R_s + j\omega_H L_d \equiv j\omega_H L_d \quad (22)$$

$$z_q = R_s + j\omega_H L_q \equiv j\omega_H L_q \quad (23)$$

In order to estimate the stator resistance and the d- axis inductance, a carrier high-frequency voltage is superimposed to the fundamental frequency voltage along the d-axis:

$$\hat{u}_{d_H} = V_H \cos(\omega_H t) \quad (24)$$

$$\hat{u}_{q_H} = 0 \quad (25)$$

and we obtain

$$\hat{i}_{d_H} = \frac{V_H \cos\omega_H t}{z_d\, z_q}\left(z_{moy} - \frac{1}{2} z_{diff} \cos 2\tilde{\theta}_e\right) \quad (26)$$

$$\hat{i}_{q_H} = -\frac{V_H \cos\omega_H t}{z_d\, z_q}\left(\frac{1}{2} z_{diff} \sin 2\tilde{\theta}_e\right) \quad (27)$$

where $z_{moy} = \frac{1}{2}(z_d + z_q)$.

The stator resistance can be identified at the steady state where the PMSM model is obtained by substituting $\dot{\hat{i}}_d = 0$ and $\dot{\hat{i}}_q = 0$ into (19). However, the d- axis inductance can be identified at transient state by using the HF model. It should be noted that with a HF voltage injection into d- axis, only L_d can be identified as the used PMSM has a low salience $\left(z_{diff} = j\omega_H(L_d - L_q) \approx 0\right)$. In this case, the q-axis current $\hat{i}_{q_H}$ is negligible and we cannot estimate L_q. The used model is then:

$$\hat{u}_{d_H} = L_d \frac{d\hat{i}_{d_H}}{dt} \quad (28)$$

To estimate the q- axis inductance, a carrier high-frequency voltage is superimposed to the fundamental frequency voltage along the q- axis. So we obtain the following equations:

$$\hat{u}_{d_H} = 0, \quad (29)$$

$$\hat{u}_{q_H} = V_H \cos\omega_H t, \quad (30)$$

$$\hat{i}_{d_H} = \frac{V_H \cos\omega_H t}{z_d\, z_q}\left(-\frac{1}{2} z_{diff} \sin 2\tilde{\theta}_e\right), \quad (31)$$

$$\hat{i}_{q_H} = \frac{V_H \cos\omega_H t}{z_d\, z_q}\left(z_{moy} + \frac{1}{2} z_{diff} \sin 2\tilde{\theta}_e\right). \quad (32)$$

In this case, the d- axis current $\hat{i}_{d_H}$ is negligible and we cannot estimate L_d. The used model is then:

$$\hat{u}_{q_H} = L_q \frac{d\hat{i}_{q_H}}{dt} \quad (33)$$

Therefore, the model can be given by

$$\begin{cases} \hat{u}_d = \hat{R}_s i_d, \\ \hat{u}_{d_H} = \hat{L}_d \dfrac{d\hat{i}_{d_H}}{dt}, \\ \hat{u}_{q_H} = \hat{L}_q \dfrac{d\hat{i}_{q_H}}{dt}. \end{cases} \quad (34)$$

At first step, we suppose that we calculate the current derivatives softly. So the general formulation of the recursive least squares (RLS) algorithm used in this paper can be presented as follows:

$$P_k = P_{k-1} - P_{k-1}\underline{\varphi}_k\left(1 + \underline{\varphi}_k^T P_{k-1}\underline{\varphi}_k\right)^{-1}\underline{\varphi}_k^T P_{k-1} \quad (35)$$

$$\underline{K}_k = P_{k-1}\underline{\varphi}_k\left(1 + \underline{\varphi}_k^T P_{k-1}\underline{\varphi}_k\right)^{-1} \quad (36)$$

$$\underline{\hat{\Theta}}_k = \hat{\Theta}_{k-1} + \underline{K}_k\left(y_k^* - \underline{\varphi}_k^T \underline{\hat{\Theta}}_{k-1}\right) \quad (37)$$

where $\underline{\hat{\Theta}} = [\hat{R}_s \quad \hat{L}_d \quad \hat{L}_q]^T$ is an estimation of $\underline{\Theta} = [R_s \quad L_d \quad L_q]^T$ and y_k^* is the measured output $\left(y_k^* = y_k + b_k\right)$; b_k is the noise which variance is equal to σ^2. P_0 and $\underline{\Theta}_0$ are the initial values of P_k and $\underline{\hat{\Theta}}_k$. If we have no information about the system, we choose $\underline{\Theta}_0 = 0$. The expression of P_k is provided by the following equation:

$$P_k = \left[\sum_{i=1}^{k} \varphi_i \varphi_i^T\right]^{-1} = \left(\phi^T \phi\right)^{-1} \quad (38)$$

with

$$\phi = \begin{bmatrix} \varphi_1^T \\ \varphi_2^T \\ \vdots \\ \varphi_K^T \end{bmatrix} = \begin{bmatrix} \varphi_{11} & \varphi_{12} & \cdots & \varphi_{1N} \\ \varphi_{21} & \varphi_{22} & \cdots & \varphi_{2N} \\ \vdots & \vdots & \ddots & \vdots \\ \varphi_{K1} & \varphi_{K2} & \cdots & \varphi_{KN} \end{bmatrix}$$

The main diagonal of P_k represents the parameters variance given with an accuracy of σ^2. If we have any information about Θ, then, its variance is infinite and we choose

$$P_0 = \alpha I = \begin{bmatrix} \alpha & 0 & \cdots & 0 \\ 0 & \alpha & \cdots & 0 \\ \vdots & \vdots & \ddots & \vdots \\ 0 & 0 & \cdots & \alpha \end{bmatrix} \quad (39)$$

with $\alpha >> 1$. By choosing α small, it means that some degree of confidence is granted to Θ_0 and the parameter variation is slow. At the limit, if $\alpha = 0$, then Θ_k is constant. The parameters are estimated one after the other which simplifies the algorithm given by (35)–(37) by avoiding the matrix inversion. The algorithm used for each parameter can be described as follows:

$$\begin{cases} P_{R,k} = P_{R,k-1} - \dfrac{\left(P_{R,k-1}\hat{i}_d\right)^2}{1+P_{R,k-1}\hat{i}_d^2} \\ K_{R,k} = \dfrac{P_{R,k-1}\hat{i}_d}{1+P_{R,k-1}\hat{i}_d^2} \\ \hat{R}_{s,k} = \hat{R}_{s,k-1} + K_{R,k}\left(\hat{u}_d - \hat{i}_d\,\hat{R}_{s,k-1}\right) \end{cases} \quad (40)$$

$$\begin{cases} P_{1,k} = P_{1,k-1} - \dfrac{\left(P_{1,k-1}\dot{\hat{i}}_{d_H}\right)^2}{1+P_{1,k-1}\dot{\hat{i}}_{d_H}^2} \\ K_{1,k} = \dfrac{P_{1,k-1}\dot{\hat{i}}_{d_H}}{1+P_{1,k-1}\dot{\hat{i}}_{d_H}^2} \\ \hat{L}_{d,k} = \hat{L}_{d,k-1} + K_{1,k}\left(\hat{u}_{d_H} - \dot{\hat{i}}_{d_H}\,\hat{L}_{d,k-1}\right) \end{cases} \quad (41)$$

$$\begin{cases} P_{2,k} = P_{2,k-1} - \dfrac{\left(P_{2,k-1}\dot{\hat{i}}_{q_H}\right)^2}{1+P_{2,k-1}\dot{\hat{i}}_{q_H}^2} \\ K_{2,k} = \dfrac{P_{2,k-1}\dot{\hat{i}}_{q_H}}{1+P_{2,k-1}\dot{\hat{i}}_{q_H}^2} \\ \hat{L}_{q,k} = \hat{L}_{q,k-1} + K_{2,k}\left(\hat{u}_{q_H} - \dot{\hat{i}}_{q_H}\,\hat{L}_{q,k-1}\right) \end{cases} \quad (42)$$

where

$$P_{R,k-1}=\alpha_R, P_{1,k-1}=\alpha_{L_d}, P_{2,k-1}=\alpha_{L_q}, \hat{R}_{s,k-1}=0, \hat{L}_{d,k-1}=0, \hat{L}_{q,k-1}=0$$

To estimate L_d and L_q, we must have the measure of the voltage u_{d_H} and u_{q_H} and calculate the current derivatives $\dot{i}_{d_H}$ and $\dot{i}_{q_H}$ respectively. The computing of these derivatives can be a source of problems if the measurement of such currents is noisy. A solution for a safe computation of these derivatives is proposed in Section 4.3. Fig. 2 shows the progress of parameters identification at standstill, the startup of the motor and the low-speed operation. Initially, we impose a zero velocity to the speed loop and a carrier high-frequency voltage is injected into the d-axis. During the first half second of the injection, the initial rotor position of the motor is estimated. At that moment, we buckle with the estimated speed while keeping the injection of the HF voltage into the d-axis. Between *t=1s* and *t=2.5s*, we estimate the stator resistance R_s and the d-axis inductance L_d using the recursive least squares method. To identify the stator resistance, we use the steady-state measurements of voltages and currents. However, the HF measurements of voltages and currents are used to estimate L_d. At *t=3*, we stop the injection into the d-axis and we inject the same HF signal into the q-axis. The stator inductance L_q is estimated between *t=4s* and *t=5.5s*.

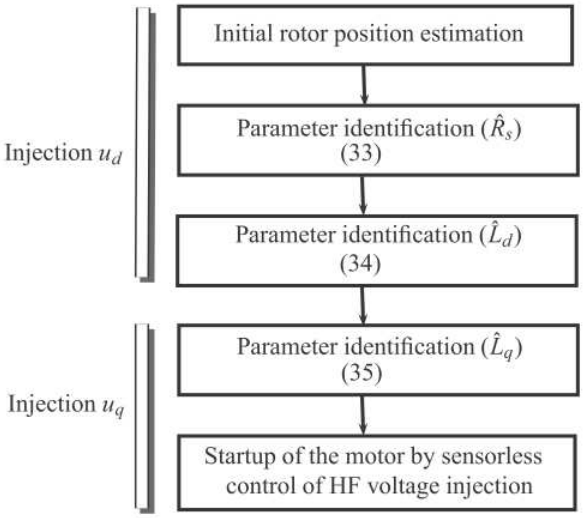

Fig. 2. Flow of parameter identification and low speeds operation.

IV. MODEL VALIDATION

A. *Simulation results*

In order to be validated, the soft sensor must provide good speed measurements for all the operating points of the motor. The synchronous motor is driven through a Field Oriented Control (FOC) with a model expressed in the rotating frame $(d-q)$. The speed controller imposes the rotor speed $\omega_m = \omega_m^*$ whatever the load torque is provided by the DC motor. PI controllers are used for the control of the currents. The soft sensor provides the speed and position estimates $\hat{\omega}_e$ and $\hat{\theta}_e$ which are used in Park's transformation.

A SPMSM, whose parameters are shown in Table. I, is used for simulation tests. The proposed soft sensor is simulated with Matlab/Simulink and it is tested according to industrial test trajectories given by Fig 3. It can be shown in Fig. 4 that the soft sensor does not provide correct estimation in the whole speed range at nominal torque. In particular, the model diverges from real value at low speed around $\omega_m = 0$. This problem around the zero speed can be explained by the fact that this soft sensor is a model-based sensor. Then, the rotor position estimation depends necessarily on the back-electromotive forces which are proportional to the PMSM speed. So, at low speeds the amplitude of these forces is insignificant which does not allow a perfect estimation of the rotor position. As a solution, HF-based sensors are used at low speed and give a good results as it exploits the saliency of the machine.

Table I. Nominal parameters of synchronous machine

Features	**Values**
Pole pair	*3*
d-axis inductance	*0.77e-3 mH*
q-axis inductance	*0.77e-3 mH*

Stator resistance	*0.2525 Ω*
Permanent magnet flux	*0.075 Wb*

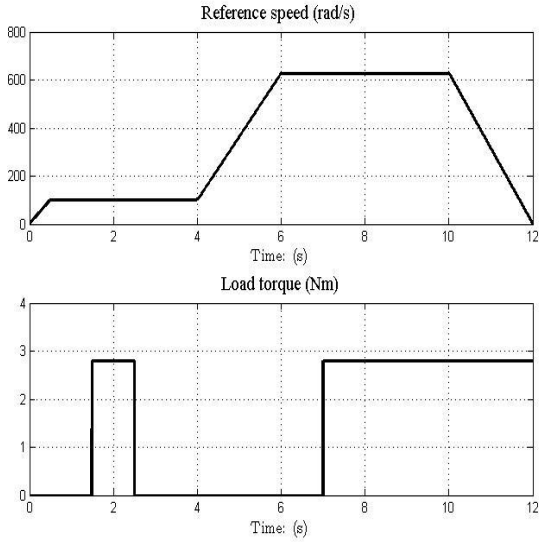

Fig 3. The reference trajectories

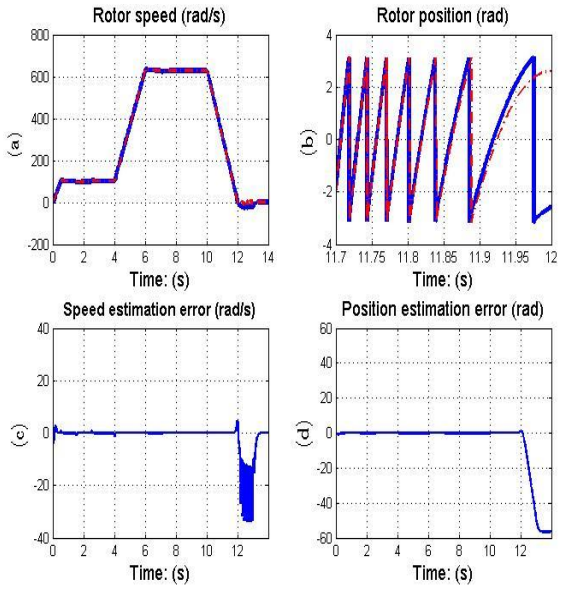

Fig. 4. Soft sensor performances: (a) actual and estimated rotor speed (b) actual and estimated rotor position (c) speed estimation error (d) position estimation error.

B. *HF-based sensor*

The HF-based sensor presented in this section used a carrier high frequency excitation. There are two main forms of carrier high frequency excitation [27]: rotating vector [28] and pulsating vector [29]. The first form injects a balanced three-phase voltage or current carrier signal. If the injected signal is a voltage, then the carrier current response consists of two components: the first one is a positive sequence component which turns in the same direction as the injected voltage vector and the second one is a negative sequence component which turns in the opposite direction. Only the negative component contains the rotor position information. It is necessary to use an appropriate signal processing to extract this component and then estimate the rotor position of the motor. In [30], a simple technique to extract the negative frequency component of the current using only one analog filter is presented. The rotating carrier injection is given by the following equation:

$$\begin{bmatrix} u_{d_H} \\ u_{q_H} \end{bmatrix} = V_H \begin{bmatrix} \cos(\omega_H t) \\ \sin(\omega_H t) \end{bmatrix} \tag{43}$$

The carrier current response along the q-axis is then given by:

$$\hat{i}_{q_H} = -\frac{V_H \sin 2\tilde{\theta}_e}{2\omega_H L_d L_q}\left(L_{diff}\sin(\omega_H t)\right) \tag{44}$$

where $\hat{i}_{q_H}$ depends on the position error $\tilde{\theta}_e$, so a synchronous demodulation is required to calculate the proportional signal to the estimation error of the rotor position. The use of analog filters allows the isolation of the term that contains information about the position and the elimination of undesirable terms. In general, the diagram can be given by Fig. 5. The band pass filter (BPF) is centered on the carrier frequency f_H. The resulting current is then multiplied by $\sin(\omega_H t)$. At the end, a low pass filter is used to get back the signal $i_{\tilde{\theta}_e}$ approached by the following equation:

$$i_{\tilde{\theta}_e} \approx -\frac{V_H L_{diff}}{2\omega_H L_d L_q}\tilde{\theta}_e \tag{45}$$

Finally, the rotor speed can be estimated using a PI controller as in [31]

$$\hat{\omega}_e = \chi_p i_{\tilde{\theta}_e} + \chi_i \int i_{\tilde{\theta}_e} dt \tag{46}$$

where χ_p and χ_i are the proportional and integral gains of the controller, respectively. The rotor position estimate is given by

$$\hat{\theta}_e = \int \hat{\omega}_e dt \tag{47}$$

C. *Computing time derivatives using state variable filters*

As shown in Fig.5, in the injection techniques, the measurements are filtered by a band pass filter (BPF) to keep the HF components only. So the idea is to simulate the BPF as a state variable filter (SVF) in order to obtain a safe computation of the current derivatives (Section 3). This filter structure is used for the determination of the current derivatives and therefore the identification of the motor parameters, as well as for the estimation of rotor position and speed in low speed (HF soft sensor). To do this, we consider the BPF given by the following equation:

$$H(p) = \frac{i_f(p)}{i(p)} = \frac{b_0 p}{a_0 + a_1 p + a_2 p^2} = \frac{\tau_2 p}{a_0 + \tau_2 p + \tau_1 \tau_2 p^2} \tag{48}$$

This filter can be simulated as a SVF which can be represented by Fig. 6 where $I_2 = \frac{1}{\tau_1 p} I_1$ and $I_3 = \frac{1}{\tau_2 p} I_2$.

With this representation, we have $I_2 = i_f$ and $I_1 = \dot{i}_f$. Therefore, the SVF allows us to filter $i(t)$ and to recover

directly $i_f(t)$ and $\dot{i}_f(t)$ using only integrators. By applying the same filter to the voltage $u(t)$, we can identify $L\left(u_f = L\dot{i}_f\right)$.

The time constants τ_1 and τ_2 must be calculated according to the characteristics of the BPF (center frequency and bandwidth). The center frequency of this filter corresponds to the frequency of injection.

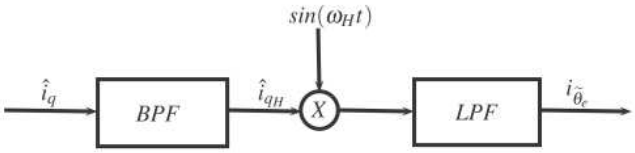

Fig. 5. Demodulation scheme used to obtain the position error signal.

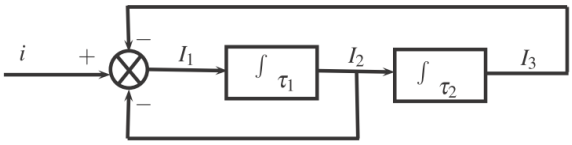

Fig. 6. Block diagram of the state variable filter.

D. Soft sensor design for real-time estimation in a wide speed range including standstill

We have presented above two soft sensors operating in two different ranges of speed. Therefore, it remains to establish a method of transition between both to get a sensorless control in the full-speed range of the permanent magnet synchronous machine.

In this section, we adopt the following notations: $\hat{\omega}_e^{LS}$ and $\hat{\theta}_e^{LS}$ are the estimated speed and position at low speed, respectively, $\hat{\omega}_e^{HS}$ and $\hat{\theta}_e^{HS}$ are the estimated speed and position at high speed, respectively, and $\hat{\omega}_e^{T}$ and $\hat{\theta}_e^{T}$ are the estimated speed and position given by the hybrid observer, respectively. The transition between the two observers, adopted in this paper, has been realized by using weight coefficients W_L and W_H. W_L prevails completely below *80 rpm*. However, W_H predominates above *100 rpm*.

To determine these coefficients, we tested the performances of the two soft sensors separately. As shown in Fig. 4, the model-based soft sensor does not provide correct estimation at low speed. So we can choose $W_H = 100$. Below *80 rpm*, the high frequency soft sensor gives good results so we select $W_L = 80$. The crossing of both algorithms do not affect the estimate of the position, since W_L and W_H are chosen such that $W_L + W_H = 1$, which leads the linear combination to be convex (Fig. 7) :

$$\hat{\omega}_e^{T} = W_H\,\hat{\omega}_e^{HS} + W_L\,\hat{\omega}_e^{LS} \quad (49)$$

$$\hat{\theta}_e^{T} = W_H\,\hat{\theta}_e^{HS} + W_L\,\hat{\theta}_e^{LS} \quad (50)$$

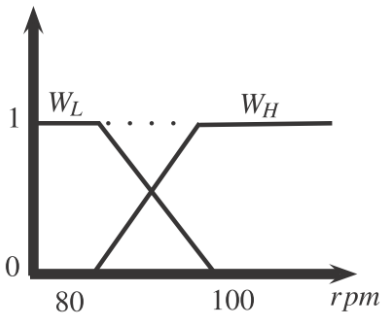

Fig. 7. The transition method.

V. Simulation Results

The proposed hybrid sensor was investigated in simulation. High frequency signal injection was activated from the standstill until *80 rpm* to estimate the position and the speed at low speed, between *80* and *100 rpm* a smooth transition was imposed. Beyond *100 rpm* the injected signal was removed and only the model-based sensor is used. Simulation results show the relevancy of the proposed hybrid soft sensor. The position estimation error is very low as shown in Fig. 8. It can be concluded that this soft sensor is simple, efficient and a suitable candidate for practical implementation.

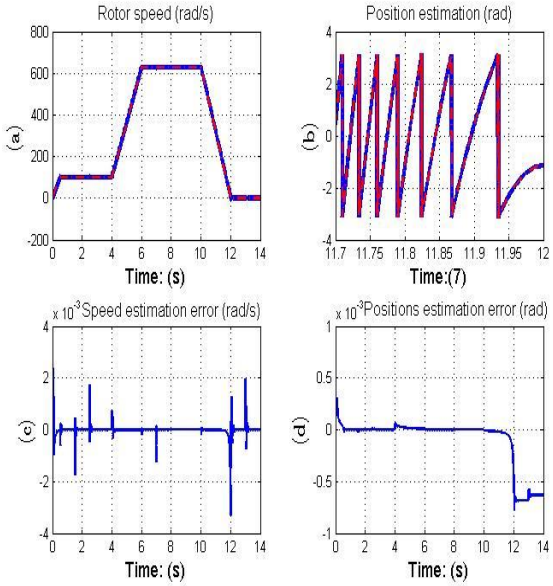

Fig. 7. Simulation results: (a) actual and estimated rotor speed (b) actual and estimated rotor position (c) speed estimation error (d) position estimation error.

VI. Conclusion

In this paper, we have presented the complete design of a soft sensor for speed measurement of permanent magnet synchronous. A reduced-order observer based upon classical concepts introduced by Luenberger for PMSM have been used at high speed. Position estimate was, then, derived from the speed estimate by integration. This observer ensures that the speed and the position estimation errors converge to zero. The interest of this observer is that there is only one parameter to be determined besides it allows to estimate the speed without stator currents estimation unlike other observers.

High-frequency soft sensor is used at low speed. Also, a method of transition between both has been presented. Simulation results showed the robustness of the proposed soft sensor.

REFERENCES

[1] R. Abdelli, D. Rekioua, T. Rekioua (2011). "Performances improvements and torque ripple minimization for VSI fed induction machine with direct control torque". *ISA Trans*, Vol. 50, Iss. 2, p.p. 213-219.

[2] A.Y. Achour, B.Mendil, S. Bacha, I. Munteanu (2009). "Passivity-based current controller design for a permanent-magnet synchronous motor". *ISA Trans*, Vol. 48, Iss. 3, p.p. 336-346.

[3] B. Zhang, Y. Pi, Y. Luo (2012). "Fractional order sliding-mode control based on parameters auto-tuning for velocity control of permanent magnet synchronous motor". *ISA Trans*, Vol. 51, Iss. 5, p.p. 649-656.

[4] Ph. Bogaerts, A. VandeWouwer (2003). "Software sensors for bioprocesses". *ISA Trans*, Vol. 42, Iss. 4, p.p. 547-558.

[5] R. F. Escobar, C. M. Astorga-Zaragoza, A. C. Tellez-Anguiano, D. Juarez-Romero, J. A. Hernandez, G. V. Guerrero-Ramirez (2011). "Sensor fault detection and isolation via high-gain observers: application to a double-pipe heat exchanger". *ISA Trans*, Vol. 50, Iss. 3, p.p. 480-486.

[6] S. R. Vijaya Raghavan, T. K. Radha krishnan, K. Srinivasan (2011). "Soft sensor based composition estimation and controller design for an ideal reactive distillation column". *ISA Trans*, Vol. 50, Iss. 1, p.p. 61-70.

[7] H. Kubota, K. Matsuse (1993). "DSP-based speed adaptive flux observer of induction motor". *IEEE Trans Ind Appl*, Vol. 29, Iss. 2, p.p. 344–348.

[8] H. R. Karimia, A. Babazadehb (2005). "Modeling and output tracking of transverse flux permanent magnet machines using high gain observer and RBF neural network". *ISA Trans*, Vol. 44, Iss. 4, p.p. 445-456.

[9] M. Hinkkanen, M. Harnefors, J. Luomi (2010). "Reduced-order flux observers with stator-resistance adaptation for speed-sensorless induction motor drives". *IEEE Trans Power Electron*, Vol. 25, Iss. 5, p.p. 1173-1183.

[10] S. Zheng, X. Tang, B. Song, S. Lu, B. Ye (2013). "Stable adaptive PI control for permanent magnet synchronous motor drive based on improved JITL technique". *ISA Trans*, Vol. 52, Iss. 4, p.p. 539-549.

[11] G. Yang, T. Chin (1993). "Adaptive-Speed identification scheme for a vector-controlled speed sensorless inverter-induction motor drive". *IEEE Trans Ind Appl*, Vol. 29, Iss. 4, p.p. 820-825.

[12] G. Madadi-Kojabadi (2005). "Simulation and experimental studies of model reference adaptive system for sensorless induction motor drive". *Simul Model Pract Theory*, Vol. 13, Iss. 6, p.p. 451-464.

[13] T. Orlowska-Kowalska, M. Dybkowski (2010). "Stator-current-based MRAS estimator for a wide range speed-sensorless induction-motor drive". *IEEE Trans Ind Electron*, Vol. 57, Iss. 4, p.p. 1296-1308.

[14] D. Xu, S. Zhang, J. Liu (2013). "Very-low speed control of PMSM based on EKF estimation with closed loop optimized parameters". *ISA Trans*, Vol. 52, Iss. 6, p.p. 835-843.

[15] I. Omrane, E. Etien, W. Dib, O. Bachelier (2015). "Modeling and simulation of soft sensor design for real-time speed and position estimation o PMSM". *ISA Trans*, Vol. 57, p.p. 329-339.

[16] F. M. DeBelie, P. Sergeant, J. A. Melkebeek (2010). "A sensorless PMSM drive using modified high-frequency test pulse sequences for the purpose of a discrete-time current controller with fixed sampling frequency". *J Math Comput Simul*, Vol. 81, Iss. 2, p.p. 367-381.

[17] R. Leidhold (2011). "Position sensorless control of PM synchronous motors based on zero-sequence carrier injection". *IEEE Trans Ind Electron*, Vol. 58, Iss. 12, p.p. 5371-5379.

[18] J. Jang, S. Sul, J. Ha, K. Ide, M. Sawamura (2003). "Sensorless drive of surface-mounted permanent-magnet motor by high-frequency signal injection based on magnetic saliency". *IEEE Trans Ind Appl*, Vol. 39, p.p. 1031-1039.

[19] C. H. Choi, J. K. Seok (2008). "Pulsating signal injection-based axis switching sensorless control of surface-mounted permanent-magnet motors for minimal zero-current clamping effects". *IEEE Trans Ind Appl*, Vol. 44, Iss. 6, p.p. 1741-1748.

[20] A. Piippo, M. Hinkkanen, J. Luomi (2009). "Adaptation of motor parameters in sensorless PMSM drives". *IEEE Trans Ind Appl*, Vol. 45, Iss. 1, p.p. 203-212.

[21] S. Sayeef, G. Foo, M. F. Rahman (2010). "Rotor position and speed estimation of a variable structure direct-torque-controlled IPM synchronous motor drive at very low speeds including standstill". *IEEE Trans Ind Electron*, Vol. 57, Iss. 11, p.p. 3715-3723.

[22] I. Omrane, W. Dib, E. Etien, O. Bachelier (2013). "Sensorless control of PMSM based on a nonlinear observer and a high-frequency signal injection for automotive applications. The 39th annual conference of the IEEE industrial electronics society IECON, Vienna, Austria, p.p. 3130-3135.

[23] J. I. Ha, S. J. Kang, S. K. Sul (2006). "Position-controlled synchronous reluctance motor without rotational transducer". *IEEE Trans Ind Appl*, Vol. 35, p.p. 1393-1398.

[24] S. Bolognani, A. Faggion, E. Fornasiero, L. Sgarbossa (2012). "Full speed range sensorless IPM motors drives". International conference on electrical machines ICEM, Marseille, France, p.p. 2209-2215.

[25] C. Silva, G. M. Asher, M. Sumner (2006). "Hybrid rotor position observer for wide speed-range sensorless PM motor drives including zero speed". *IEEE Trans Ind Electron*, Vol. 53, Iss. 2, p.p. 373-378.

[26] A. Barakat, S. Tnani, G. Champenois, E. Mouni (2010), "Analysis of synchronous machine modeling for simulation and industrial applications", *Journal of Simulation Modeling Practice and Theory*, Vol. 18, Iss. 9, pp. 1382 – 1396.

[27] P. Garcia, J. M. Guerrero, I. El-Sayed, F. Briz, D. Reigosa (2010). "Carrier signal injection alternatives for sensorless control of active magnetic bearings". Symposium on sensorless control for electrical drives SLED, Padova, Italy, p.p. 78-85.

[28] M. Linke, R. Kennel, J. Holtz (2002). "Sensorless position control of permanent magnet synchronous machines without limitation at zero speed". The 28th annual conference of the IEEE industrial electronics society IECON, Sevilla, Spain, p.p. 674-679.

[29] W. Hammel, R. M. Kennel (2010). "Position sensorless control of PMSM by synchronous injection and demodulation of alternating carrier voltage". Symposium on sensorless control for electrical drives SLED, Padova, Italy, p.p. 56-63.

[30] O. Mansouri-Toudert, H. Zeroug, F. Auger, A. Chibah (2012). "Improved rotor position estimation of salient-pole PMSM using high frequency carrier signal injection". International conference on electrical machines ICEM, Marseille, France, p.p. 761-767.

[31] A. Piippo, M. Hinkkanen, J. Luomi (2009). "Adaptation of motor parameters in sensorless PMSM drives". *IEEE Trans Ind Appl*, Vol. 45, Iss. 1, p.p. 203-212.